Colloid Polym Sci (2007) 285:1699–1705
DOI 10.1007/s00396-007-1747-0

SHORT COMMUNICATION

Analysis of dynamic surface tension of tetraethyleneglycol monooctyl ether at air/water interface

Saeid Azizian · Hitomi Motani · Kinue Shibata · Takashi Matsuda · Takanori Takiue · Hiroki Matsubara · Makoto Aratono

Received: 12 June 2007 / Revised: 12 July 2007 / Accepted: 18 July 2007 / Published online: 14 August 2007

Abstract The dynamic surface tension of the aqueous solutions of tetraethyleneglycol monooctyl ether (C_8E_4), a nonionic surfactant, was measured at different concentrations and temperatures. Present data at 298.15 K clearly indicate that the mechanism of adsorption is purely diffusion controlled at low concentrations (0.1~0.4 mmol/kg), and there is a switchover in adsorption mechanism to the mixed diffusion-kinetic control at higher concentrations. The calculated activation energies increase with concentration, and thus, with surface density, but decrease with temperature. The magnitude of activation energy and its increase with surface density suggest that the barrier is due to the free surface site formation by overcoming mainly the attractive van der Waals forces between the chain of adsorbed C_8E_4 molecules.

Keywords Dynamic surface tension · Adsorption kinetics · C_8E_4 · Nonionic surfactant

Introduction

Generally, a surfactant solution is characterized by the surface tension and adsorption of surfactant molecules at the solution interface with another fluid. When the interface is not at equilibrium, the measured surface tension is referred to dynamic surface tension. By both equilibrium and dynamic surface tension measurements, significant information on the state of adsorbed film and its transition have been obtained [1–6]. Although during the last decades interfacial phenomena have been a chief object of several theoretical and experimental investigations, studies of dynamic behavior of surface tension seems to be insufficient, both from theoretical and experimental point of view. The rate of surfactant adsorption has crucial importance for some processes including wetting, coating, foaming [7], breathing [8, 9], washability [10], enhanced oil recovery [11]. For example, an ink with good wettability and good print quality not only should have a low equilibrium surface tension but also its dynamic surface tension should decrease rapidly with time; thus, dynamic surface tension provides a modern tool for clever selection of appropriate dispersants with a good dynamic wetting behavior. In addition, the designers of aerosol dispersing systems may perform dynamic surface tension measurements to optimize nozzle design. Dynamic surface tension measurements have been demonstrated as a tool for characterizing lung surfactants too. Dynamic surface tension measurement is a powerful technique for the study of surface phase transition [6, 12]. A comprehensive study on adsorption dynamics of 1-decanol as a nonionic surfactant at air/water interface has been reported by Lin et al. [13]. Furthermore, several reviews in recent years on surfactant adsorption dynamics reveal the importance of study of dynamic surface tension [14–17].

It was shown experimentally that for some dilute solutions, the adsorption kinetics is controlled by molecular diffusion from the bulk to the interface. By using dynamic surface tension data, it is possible to find the adsorption mechanism of surfactant from bulk to the interface.

S. Azizian · H. Motani · K. Shibata · T. Matsuda · T. Takiue · H. Matsubara · M. Aratono (✉)
Department of Chemistry, Faculty of Sciences,
Kyushu University,
Hakozaki 6-10-1,
Higashiku, Fukuoka 812-8581, Japan
e-mail: m.arascc@mbox.nc.kyushu-u.ac.jp

S. Azizian (✉)
Faculty of Chemistry, Bu-Ali Sina University,
Hamadan, Iran
e-mail: sazizian@basu.ac.ir

The purpose of the present work was to investigate the adsorption of C_8E_4, a nonionic surfactant, at air/water interface from both equilibrium and kinetic point of view.

Experimental

Materials

Tetraethyleneglycol monooctyl ether (C_8E_4) purchased from BACHEM Feinchemikalien AG was purified by three-phase extraction technique (3PHEX) [18]. The purity of C_8E_4 was checked by observing no minimum around the critical micelle concentration (CMC) on the surface tension vs concentration curve. Water was distilled three times from dilute alkaline permanganate solution.

Surface tension measurements

Dynamic surface tension $\gamma(t)$ of the aqueous solutions of C_8E_4 was measured by use of the automatic measurement device based on the pendant drop method at different bulk concentrations at 298.15 K under atmospheric pressure. For the temperature effect on $\gamma(t)$, $\gamma(t)$ was measured at given equilibrium surface densities from 288.15 to 308.15 K at interval of 2.5 K under atmospheric pressure. The experimental error of surface tension was within ±0.05 mN/m. $\gamma(t)$ was measured at concentrations below the CMC to eliminate any possible effects attributable to micelles.

Theory

The Ward–Todari equation [19] is a well-known one for describing the time dependency of adsorption:

$$\Gamma^H(t) = 2C_0\left(\frac{Dt}{\pi}\right)^{1/2} - 2\left(\frac{D}{\pi}\right)^{1/2}\int_0^t C_S(t-\tau)d\tau^{1/2} \quad (1)$$

where C_0 and C_S are bulk and subsurface concentrations of surfactant, respectively, D is the monomer diffusion coefficient, $\Gamma^{H}(t)$ is the dynamic surface density, and t is the time. As $t\to\infty$, the value C_S approaches the C_0 and can be regarded as constant. Thus, we have

$$\Delta C_{t\to\infty} = C_0 - C_s = \Gamma^H(t)\left(\frac{\pi}{4Dt}\right)^{1/2} \quad (2)$$

The adsorption equation at constant T and p

$$d\gamma(t) = -\frac{RT\Gamma^{H}(t)}{C_S}dC_S \quad (3)$$

and rearrangement give

$$\gamma(t)_{t\to\infty} - \gamma_{eq} = \frac{RT\left(\Gamma^{H}(t)\right)^2}{2C_S}\left(\frac{\pi}{Dt}\right)^{1/2} \quad (4)$$

where $\gamma(t)$ and γ_{eq} are dynamic and equilibrium surface tensions, respectively. It is found from Eq. 4 that the dependency of $\gamma(t)$ on time includes other time-dependent variables, i.e., C_s and $\Gamma^{H}(t)$. Although they are usually assumed to be equal to equilibrium values as [17]:

$$\gamma(t)_{t\to\infty} - \gamma_{eq} = \frac{RT\left(\Gamma^{H}_{eq}\right)^2}{2C_0}\left(\frac{\pi}{Dt}\right)^{1/2} \quad (5)$$

we develop Eq. 4 a little more strictly. To evaluate C_S and $\Gamma^{H}(t)$, although various types of equation of surface states are applicable, we employed the Langmuir equation because as will be shown later, the equilibrium data for present system show an acceptable fitting to the Langmuir isotherm:

$$\frac{\Gamma^{H}(t)}{\Gamma^{H}_{sat}} = \frac{\alpha C_S}{1+\alpha C_S} \quad (6)$$

and

$$\frac{\Gamma^{H}_{eq}}{\Gamma^{H}_{sat}} = \frac{\alpha C_0}{1+\alpha C_0} \quad (7)$$

where Γ^{H}_{sat} and Γ^{H}_{eq} are the saturated and equilibrium surface densities, respectively, and α is the constant parameter. From Eqs. 6 and 7, the relationship between C_S and $\Gamma^{H}(t)$ is obtained as

$$\frac{C_0}{C_S} = \frac{\Gamma^{H}_{eq}}{\Gamma^{H}(t)}\frac{\Gamma^{H}_{sat} - \Gamma^{H}(t)}{\Gamma^{H}_{sat} - \Gamma^{H}_{eq}} \quad (8)$$

Inserting Eq. 8 into Eq. 4 yields

$$\gamma(t)_{t\to\infty} - \gamma_{eq} = \frac{RT\left(\Gamma^{H}_{eq}\right)^2}{2C_0}\left(\frac{\pi}{(f(t))^2 Dt}\right)^{1/2} \quad (9)$$

where $f(t)$ is defined by

$$f(t) = \left\{\frac{\Gamma^{H}_{eq}}{\Gamma^{H}_{sat}}\left(1-\frac{\Gamma^{H}_{eq}}{\Gamma^{H}_{sat}}\right)\right\} \Big/ \left\{\frac{\Gamma^{H}(t)}{\Gamma^{H}_{sat}}\left(1-\frac{\Gamma^{H}(t)}{\Gamma^{H}_{sat}}\right)\right\} \quad (10)$$

Equation 9 includes only one time-dependent factor $f(t)$ determined by $\Gamma^{H}(t)$. $f(t)$ becomes unity at equilibrium

state, and thus, Eq. 9 results in Eq. 5. The remaining is how to calculate $\Gamma^{H}(t)$. This is achieved by the following way.

Inserting Eq. 6 into Eq. 3 results in

$$d\gamma(t) = -\frac{\Gamma^{H}_{sat} RT\alpha}{1+\alpha C_S} dC_S \tag{11}$$

Integrating Eq. 11, we obtain

$$\Gamma^{H}(t) = \Gamma^{H}_{sat} + \left(\Gamma^{H}_{eq} - \Gamma^{H}_{sat}\right) \exp \frac{\gamma(t)-\gamma_{eq}}{\Gamma^{H}_{sat} RT} \tag{12}$$

Equation 9 is valid for the adsorption with diffusion-controlled mechanism. However, in some conditions, the surfactant monomers cannot adsorb from subsurface without overcoming an adsorption barrier. In such cases, the mechanism is called "mixed diffusion-kinetic control". For this case, Liggieri et al. [20, 21] introduced an effective diffusion coefficient, D_E, which accounts for both diffusion from the bulk to the subsurface and then crossing a barrier to the interface, as:

$$D_E = D \exp\left(-\frac{E_a}{kT}\right) \tag{13}$$

where E_a is adsorption activation energy. For mixed diffusion-kinetic control model, Eq. 9 is converted to

$$\gamma(t)_{t\to\infty} - \gamma_{eq} = \frac{RT\left(\Gamma^{H}_{eq}\right)^2}{2C_0}\left(\frac{\pi}{(f(t))^2 D_a t}\right)^{1/2} \tag{14}$$

where D_a is apparent diffusion coefficient defined as:

$$D_a \equiv \frac{D_E^2}{D} = D \exp\left(-\frac{2E_a}{kT}\right) \tag{15}$$

Thus, the D_a values can be obtained from the slope of $\left(\gamma(t)_{t\to\infty} - \gamma_{eq}\right) f(t)$ vs $t^{-1/2}$ plot.

Results and discussion

Concentration effect on dynamic surface tension The equilibrium surface tension of aqueous C_8E_4 solutions is plotted against molality, m, at 298.15 K and atmospheric pressure in Fig. 1. This diagram shows the CMC around 8.5 mmol/kg. The surface tension decreases rapidly with increasing molality of C_8E_4 and is almost constant above the CMC. The equilibrium surface density Γ^{H}_{eq} was calculated from the equilibrium surface tension data and shown in Fig. 1. The Γ^{H}_{eq} values increase with m and reach the almost saturated value, Γ^{H}_{sat}, at the CMC. Figure 2 shows the linear form of the Langmuir plot $\left(m \Big/ \Gamma^{H}_{eq} \text{ vs } m\right)$ for present system, and as can be seen, there is an acceptable fitting of experimental data to the Langmuir equation.

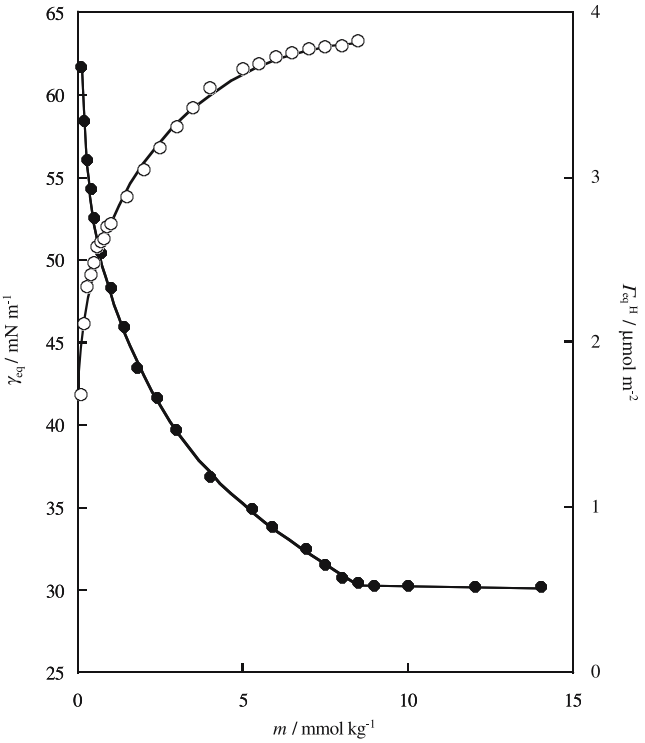

Fig. 1 γ_{eq} vs m curve of C_8E_4 at 298.15 K (*filled circles*). Γ^{H}_{eq} vs m curve of C_8E_4 at 298.15 K (*open circles*)

The $\gamma(t)$ vs time curves of C_8E_4 systems are shown in Fig. 3a. The $\gamma(t)$ values decrease very rapidly at initial stage of the adsorption and gradually with time. $\Gamma^{H}(t)$ vs t curves are obtained by applying Eq. 12 to the $\gamma(t)$ vs t curves and using the values of γ_{eq}, Γ^{H}_{eq} and Γ^{H}_{sat} given in Fig. 1. The results are shown in Fig. 3b. It is seen that $\Gamma^{H}(t)$ increases very rapidly at the initial stage of adsorption, and at the final stage of adsorption, $\Gamma^{H}(t)$ reaches Γ^{H}_{eq}. For modeling dynamic surface tension data, at first, we applied reversible formation of monolayer island model which has

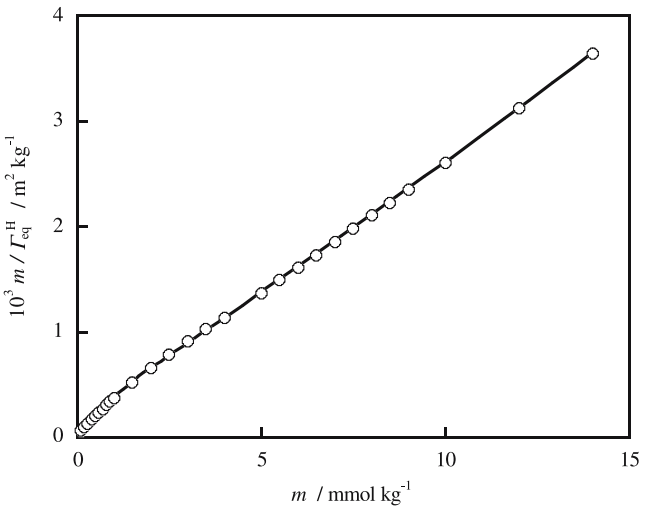

Fig. 2 Linear form of the Langmuir equation for equilibrium adsorption data of C_8E_4 at 298.15 K

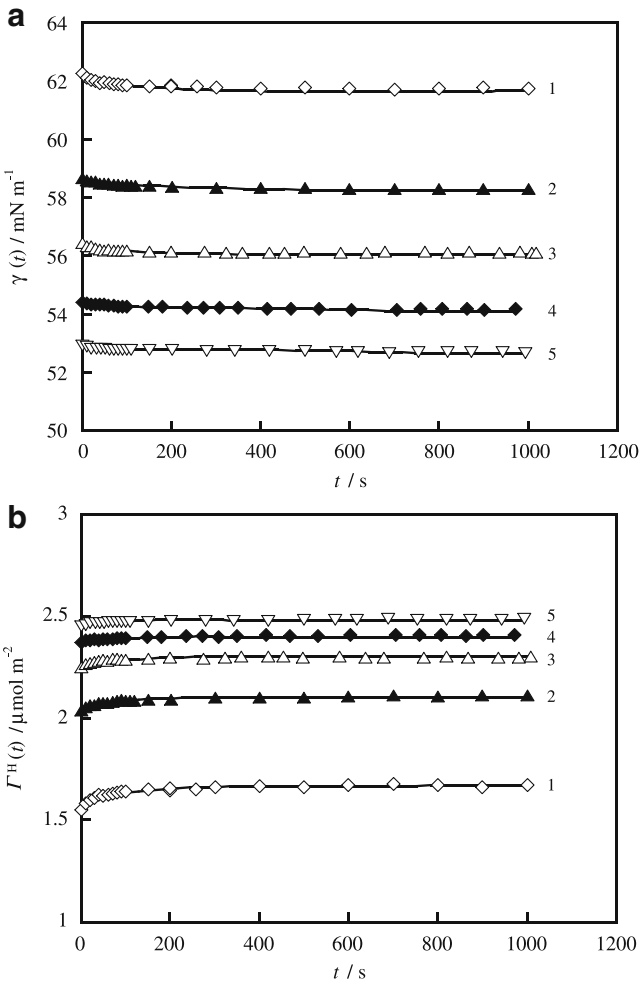

Fig. 3 **a** Dynamic surface tension $\gamma(t)$ vs time curves for C_8E_4 at 298.15 K; (*1*) m=0.1 mmol/kg, (*2*) 0.2, (*3*) 0.3, (*4*) 0.4, (*5*) 0.5. **b** Dynamic surface density $\Gamma^{H}(t)$ vs time curves for C_8E_4 at 298.15 K; (*1*) m=0.1 mmol/kg, (*2*) 0.2, (*3*) 0.3, (*4*) 0.4, (*5*) 0.5

been presented recently by Prosser et al. [22]. This kinetic model accounts for non-diffusion-controlled adsorption. By application of this model for adsorption kinetics of C_8E_4 at air/water interface, we did not find a good fitting to the experimental data, and therefore, it was concluded that the dynamic adsorption of C_8E_4 at air/water interface is not controlled by a pure non-diffusion model. Therefore, we applied diffusion-controlled and also mixed diffusion-kinetic-controlled models for the present system.

Figure 4 shows an example plot of $\left(\gamma(t)_{t\to\infty} - \gamma_{eq}\right) f(t)$ vs $t^{-1/2}$ at m=4 mmol/kg. Although the value of $f(t)$ is near to unity, we applied it in our calculations. The apparent diffusion coefficient, D_a, can be derived from its slope on the basis of Eq. 14. The important point here is selection of the data range whose slope gives a correct value of D_a. Although it is usual to employ all the data for estimating D_a, on the basis of the *Log-Log* plot of Eq. 14, we should employ only the data range shown by gray circles in Fig. 4 because only these data have slope of −1/2 in the *Log-Log*

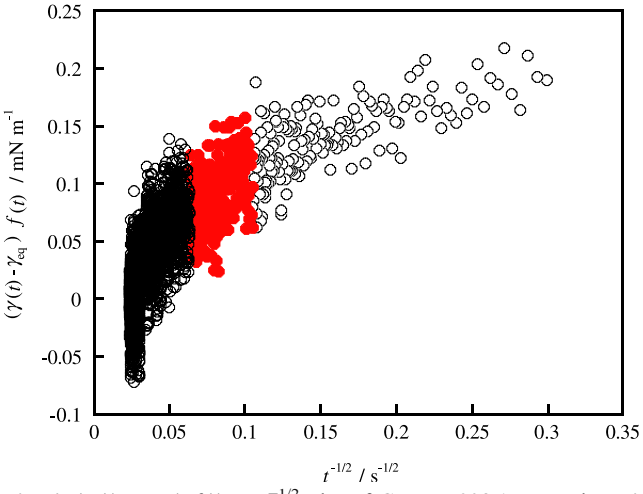

Fig. 4 $(\gamma(t) - \gamma_{eq})\, f(t)$ vs $t^{-1/2}$ plot of C_8E_4 at 298.15 K and m=4 mmol/kg

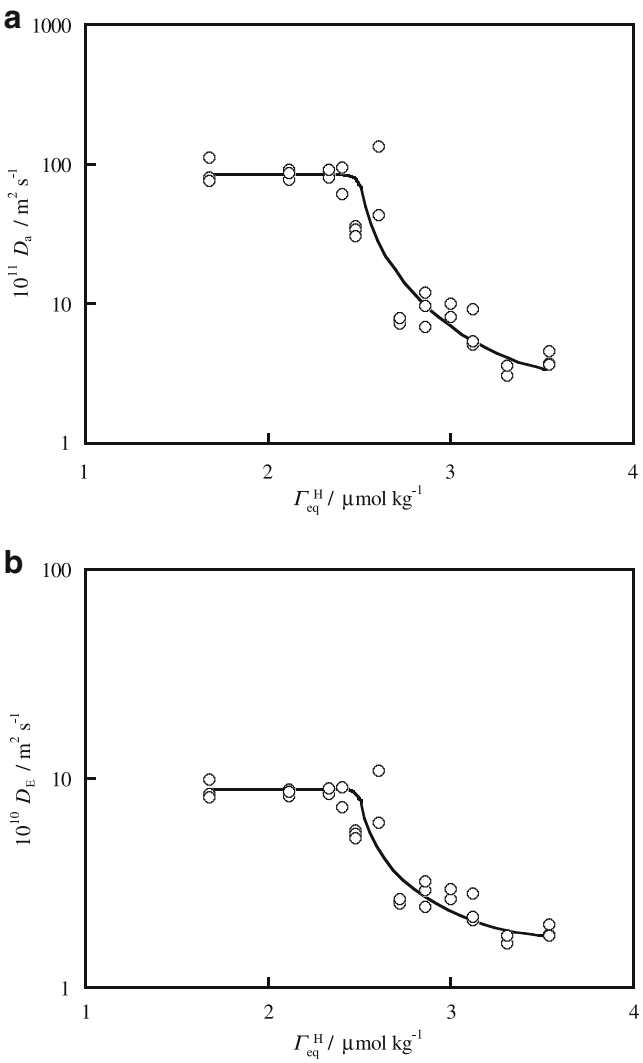

Fig. 5 **a** Apparent diffusion coefficient D_a vs Γ^{H}_{eq} for C_8E_4 at 298.15 K. **b** Effective diffusion coefficient D_E vs Γ^{H}_{eq} for C_8E_4 at 298.15 K

plot. The data in the black-like region of the left side of gray region of Fig. 4 are nearly in equilibrium because their $(\gamma(t)_{t\to\infty} - \gamma_{eq})f(t)$ function are about zero within experimental error of tensiometer (±0.05 mN/m), and therefore, it is better not to use them. On the other hand, the data presented by open circles on the right side of the gray region of Fig. 4 are also far from equilibrium and therefore cannot be used in Eq. 14 for estimation of D_a because this equation is valid at $t\to\infty$. Therefore, as *Log-Log* plot shows only the gray region, data are suitable for fitting on Eq. 14 and derivation of D_a. Finally, from the slope of $(\gamma(t)_{t\to\infty} - \gamma_{eq})f(t)$ vs $t^{-1/2}$ plot in the data range mentioned above, the D_a values have been derived.

Figure 5a shows the derived D_a values at different surface densities. This figure shows D_a is constant at low surface, and thus, also bulk concentrations, and then decreases with increasing concentration. For calculation of effective diffusion coefficient, D_E, on the basis of Eq. 15, we need the diffusion coefficient of free monomer molecule, D. The constant value of D_a at very low bulk concentrations in Fig. 5a can be regarded as the diffusion coefficient of free surfactant molecule, $D=8.77\times10^{-10}$ m^2 s^{-1}. The calculated value of D_E is plotted as a function of surface density in Fig. 5b. The D_E value is constant at low surface densities, but decreases with increasing Γ^H_{eq} at higher ones. This decrease means appearance of an activation barrier to adsorption. Now we can calculate the activation energy of adsorption, E_a, from Eq. 13. The calculated E_a is plotted against the surface density at constant temperature in Fig. 6. This figure shows E_a is zero up to $\Gamma^H_{eq} \approx 2.4$ μmol m^{-2}. This means that in this low surface concentration range, the kinetics of adsorption is controlled only by diffusion, that is, the adsorption process from subsurface to surface is fast, and there is no barrier for it. By increasing surface density, the activation barrier appears and reaches 5~6 kJ/mol at Γ^H_{sat}. The appearance and increase of activation energy with increasing Γ^H_{eq} mean that in the range of $\Gamma^H_{eq} > 2.4$ μmol m^{-2}, the rate of adsorption from subsurface to surface decreases, and thus, both diffusion (from bulk to subsurface) and adsorption (from subsurface to surface) affect the total rate of migration of surfactant molecules from bulk to surface. In other words, in this range of surface concentration, the adsorption is "mixed diffusion-kinetic control". The magnitude of activation energy and also its increase with increasing of surface density suggest that this barrier is due to the formation of free surface sites for adsorbing molecules. Maybe, the attractive van der Waals forces between the long chain of adsorbed C_8E_4 molecules at high surface densities account for barrier of free surface site formation. Although there is dehydration phenomena for adsorption of C_8E_4 at air/water interface (as will be mentioned later), at $\Gamma^H_{eq} < 2.4$ μmol m^{-2}, as the surface density is low, the contribution of dehydration activation energy seems to be ignorable, and therefore, the activation energy is about zero at $\Gamma^H_{eq} < 2.4$ μmol m^{-2}.

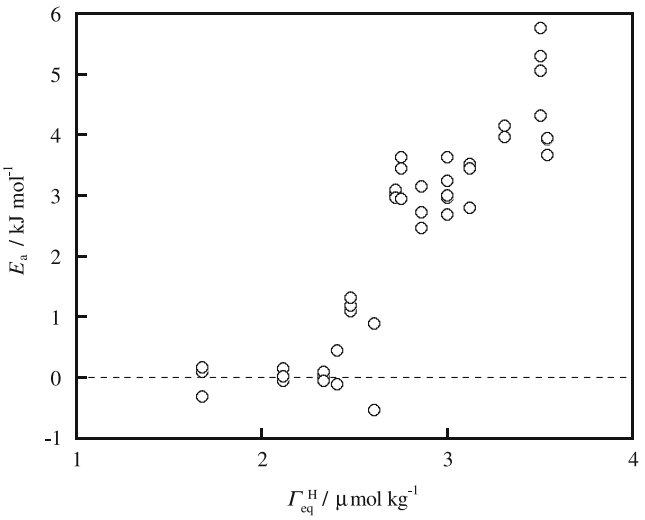

Fig. 6 Activation energy of adsorption E_a vs Γ^H_{eq} at 298.15 K

Temperature effect on dynamic surface tension In the previous section, it was demonstrated that the adsorption barrier exists at the high surface density regions. Here, we

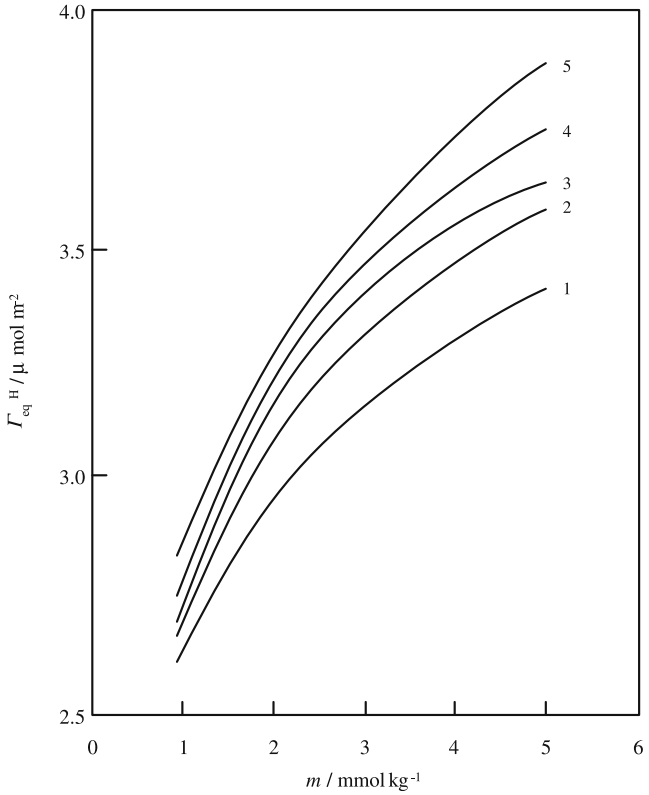

Fig. 7 Γ^H_{eq} vs m curves of C_8E_4 aqueous solution at various temperatures. (1) T=288.15 K, (2) 293.15, (3) 298.15, (4) 303.15, (5) 308.15

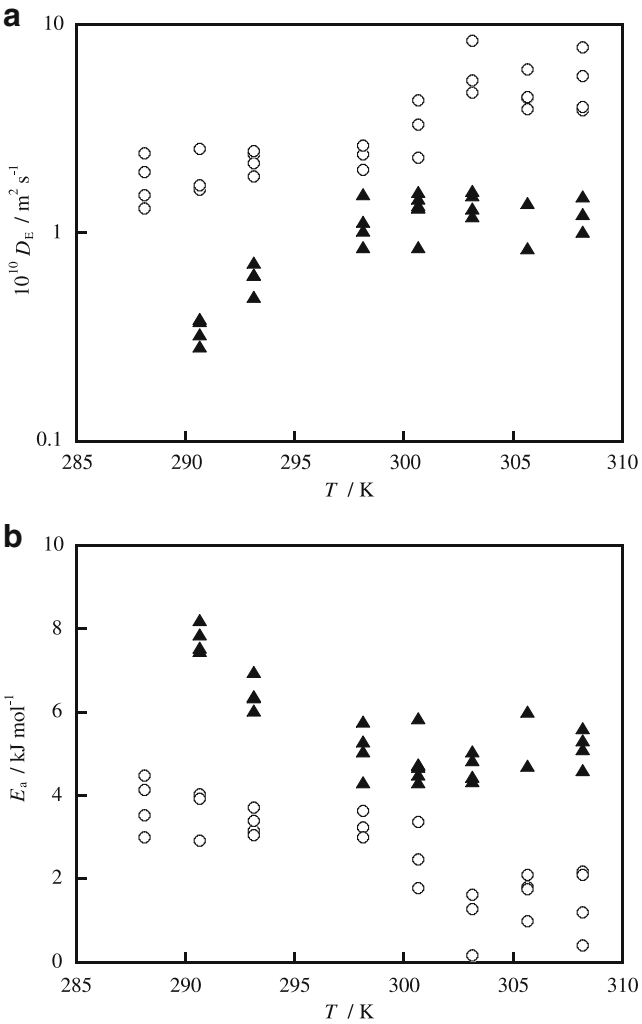

Fig. 8 **a** D_E vs temperature at constant surface densities. **b** E_a vs temperature at constant surface densities; Γ^H_{eq} =3.0 μmol m^{-2} (*open circles*), 3.5 (*filled triangles*)

measured $\gamma(t)$ at different temperatures to estimate the effect of temperature on the adsorption kinetics of C_8E_4 at the air/water interface. First, let us specify the measurement conditions. Figure 7 shows the Γ^H_{eq} vs m curves of C_8E_4 aqueous solution at various temperatures. As shown in this figure, the Γ^H_{eq} also increases with a rise in temperature, which is on opposite of usual trend. This increase of Γ^H_{eq} with temperature is due to the dehydration of head group of surfactant at higher temperatures, which leads to the reduction in head size, and therefore, the surfactant molecules can be adsorbed with closer packing. This trend has been already reported for $C_{10}E_5$ [23]. As the adsorption barrier depends on Γ^H_{eq}, the dynamic surface tension was measured under the condition of the constant surface density at Γ^H_{eq} =3.0 and 3.5 μmol m^{-2} at all temperatures.

The effective diffusion coefficient at different temperatures was calculated similarly to the previous section by using the plot of $(\gamma(t) - \gamma_{eq})f(t)$ vs $t^{-1/2}$. The values of D_E obtained are plotted against T at different surface densities in Fig. 8a. It is found that although the surface has the same Γ^H_{eq}, there is an increase in D_E value as temperature increases. The Stokes–Einstein equation

$$D = kT/6\pi\eta r \tag{16}$$

where k is Boltzmann constant, η is viscosity of solution, and r is the hydrodynamic radius suggests that D increases with temperature. In addition, Eq. 13 shows that the D_E/D value approaches unity as increasing temperature. Therefore, the adsorption process is expected to become a diffusion-controlled one at high temperatures. Figure 8b shows the calculated activation energies at different temperatures. The decrease of E_a with temperature means that the rate of adsorption from subsurface to surface increases with temperature. In other words, the free surface site formation becomes easier, even at the same surface density, due to weaker attractive van der Waals forces between the chains of adsorbed C_8E_4 molecules at higher temperatures.

Conclusion

On the basis of dynamic surface tension measurements at different concentrations of C_8E_4 and also different temperatures, the kinetics of adsorption at the air/water interface was analyzed. The results show that at low concentrations, the adsorption kinetics of C_8E_4 is purely diffusion control. At higher concentrations, the mechanism of adsorption changes to the mixed diffusion-kinetic control. This conclusion was obtained on the basis of appearance of activation energy at higher concentrations. The obtained activation energy is a function of both concentration and temperature. The magnitude of activation energy and also its change with concentration and temperature suggest that this barrier is due to free surface site formation. The origin of barrier for surface site formation is to overcome mainly the attractive van der Waals forces between the chains of adsorbed C_8E_4 molecules at air/water interface.

Acknowledgment S. Azizian acknowledges support from the Japan Society for Promotion of Science (JSPS) for providing a postdoctoral fellowship (no. P05137) at Kyushu University. This work was supported also by the Grant-in-Aid for Scientific Research(B) (No.16350075). K. Shibata also acknowledges the aid from JSPS for the present study (N0. 17.6219, DC1).

References

1. Adamson AW, Gast AP (1997) Physical chemistry of surfaces, 6th edn. Wiley, New York
2. Aratono M, Uryu S, Hayami Y, Motomura K, Matuura R (1984) J Colloid Interface Sci 98:1

3. Aratono M, Ohta A, Minamizawa H, Ikeda N, Iyota H, Takiue T (1999) J Colloid Interface Sci 217:128
4. Aratono M, Villeneuve M, Takiue T, Ikeda N, Iyota H (1998) J Colloid Interface Sci 200:161
5. Matubayasi N, Motomura K, Aratono M, Matuura R (1978) Bull Chem Soc Jpn 51:2800
6. Azizian S, Shibata K, Matsuda T, Takiue T, Matsubara H, Aratono M (2006) J Phys Chem B 10:17034
7. Dimant H, Ariel G, Andelman D (2001) Colloids Surf A 183–185:259
8. van den Tempel M, Lucassen-Reynders EH (1983) Adv Colloid Interface Sci 18:281
9. Park SY, Hannemann RE, Francess EI (1999) Colloids Surf B 15:325
10. Vandegrift AE, Rutkowski BJ (1966) J Am Oil Chem Soc 44:107
11. Miller R, Sedev R, Schano KH, Ng C, Naumann AW (1983) Colloids Surf 18:281
12. Tsay RY, Wu TF, Lin SY (2004) J Phys Chem B 108:18623
13. Lin SY, McKeigue K, Maldarelli C (1991) Langmuir 7:1055
14. Eastoe J, Rankin A, Wat R, Bain CD (2001) Int Rev Phys Chem 20:357
15. Ferri JK, Stebe KJ (2000) Adv Colloid Interface Sci 85:61
16. Chang CH, Franses EI (1995) Colloids Surf A 100:1
17. Fainerman VB, Makievski AV, Miller R (1994) Colloids Surf A 87:61
18. Schubert KV, Strey R, Kahlweit M (1991) Progr Colloid Polym Sci 84:103
19. Ward AFH, Todari L (1946) J Chem Phys 14:453
20. Liggieri L, Ravera F, Passerone A (1996) Colloids Surf A 114:351
21. Ravera F, Liggieri L, Steinchen A (1993) J Colloid Interface Sci 156:109
22. Prosser AJ, Retter U, Lunkenheimer K (2004) Langmuir 20:2720
23. Wongwailikhit K, Ohta A, Seno K, Nomura A, Shinozuka T, Takiue T, Aratono M (2001) J Phys Chem B 105:11462